Pharmacogn. Mag.
A multifaceted peer reviewed journal in the field of Pharmacognosy and Natural Products
www.phcog.com | www.phcog.net

ORIGINAL ARTICLE

Comparative Analysis of Transcriptomes of Macrophage Revealing the Mechanism of the Immunoregulatory Activities of a Novel Polysaccharide Isolated from *Boletus speciosus* Frost

Xiang Ding[1,2], Hongqing Zhu[1], Yiling Hou[1], Wanru Hou[1], Nan Zhang[1], Lei Fu[1]

[1]College of Life Sciences, Key Laboratory of Southwest China Wildlife Resources Conservation, College of Life Sciences, China West Normal University, [2]College of Environmental Science and Engineering, China West Normal University, Nanchong, Sichuan Province 637009, China

Submitted: 23-03-2016 Revised: 02-05-2016 Published: 19-07-2017

ABSTRACT

Background: The mechanism of the immunoregulatory activities of polysaccharide is still not clear. **Materials and Methods:** Here, we performed the B-cell, T-cell, and macrophage cell proliferation, the cell cycle analysis of macrophage cells, sequenced the transcriptomes of control group macrophages, and *Boletus speciosus* Frost polysaccharide (BSF-1) group macrophages using Illumina sequencing technology to identify differentially expressed genes (DEGs) to determine the molecular mechanisms of immunomodulatory activity of BSF-1 in macrophages. **Results:** These results suggested that BSF-1 could promote the proliferation of B-cell, T-cell, and macrophages, promote the proliferation of macrophage cells by abolishing cell cycle arrests in the G0/G1 phases, and promote cell cycle progression in S-phase and G2/M phase, which might induce cell division. A total of 12,498,414 and 11,840,624 bp paired-end reads were obtained for the control group and BSF-1 group, respectively, and they corresponded to a total size of 12.5 G bp and 11.8 G bp, respectively, after the low-quality reads and adapter sequences were removed. Approximately 81.83% of the total number of genes (8,257) were expressed reads per kilobase per million mapped reads (RPKM ≥1) and more than 1366 genes were highly expressed (RPKM >60) in the BSF-1 group. A gene ontology-enrichment analysis generated 13,042 assignments to cellular components, 13,094 assignments to biological processes, and 13,135 assignments to molecular functions. A Kyoto Encyclopedia of Genes and Genomes pathway enrichment analysis showed that the mitogen-activated protein kinase (MAPK) signaling pathways are significantly enriched for DEGs between the two cell groups. **Conclusion:** An analysis of transcriptome resources enabled us to examine gene expression profiles, verify differential gene expression, and select candidate signaling pathways as the mechanisms of the immunomodulatory activity of BSF-1. Based on the experimental data, we believe that the significant antitumor activities of BSF-1 *in vivo* mainly involve the MAPK signaling pathways.

Key words: Differentially expressed gene, macrophage, mechanism, polysaccharide, RNA-Seq

SUMMARY

- *Boletus speciosus* Frost-1 (BSF-1) could promote the proliferation of B-cell, T-cell, and macrophages, promote the proliferation of macrophage cells by abolishing cell cycle arrests in the G0/G1 phases, and promote cell cycle progression in S-phase and G2/M phase, which might induce cell division
- Approximately 81.83% of the total number of genes (8257) were expressed (reads per kilobase per million mapped reads [RPKM] ≥1) and more than 1366 genes were highly expressed (RPKM >60) in the BSF-1 group
- A gene ontology-enrichment analysis generated 13,042 assignments to cellular components, 13,094 assignments to biological processes, and 13,135 assignments to molecular functions
- A Kyoto Encyclopedia of Genes and Genomes pathway enrichment analysis showed that the mitogen-activated protein kinase signaling pathways are significantly enriched for DEGs between the two cell groups.

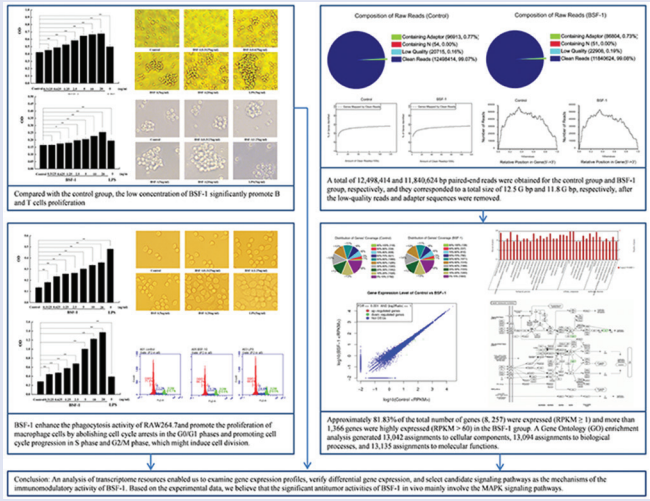

Abbreviations used: BSF-1: *Boletus speciosus* Frost polysaccharide.

Correspondence:

Prof. Yiling Hou,
Key Laboratory of Southwest China Wildlife Resources Conservation,
College of Life Sciences,
China West Normal University, Nanchong,
Sichuan Province 637009, China.
E-mail: biostart8083@126.com

DOI: 10.4103/pm.pm_151_16

Access this article online
Website: www.phcog.com
Quick Response Code:

INTRODUCTION

Recently, polysaccharides obtained from microorganisms, fungi, and plants have been regarded as the most effective immune-regulating substances, and they have been shown to be clinically effective. Polysaccharides have anti-inflammatory, antihypoglycemic, antibacterial, and antitumor activities, and the basic mechanisms underlying the therapeutic effects of fungal polysaccharides, including their antitumor and immunostimulatory activities, likely occur through the modulation

Cite this article as: Ding X, Zhu H, Hou Y, Hou W, Zhang N, Fu L. Comparative analysis of transcriptomes of macrophage revealing the mechanism of the immunoregulatory activities of a novel polysaccharide isolated from *Boletus speciosus* frost. Phcog Mag 2017;13:463-71.

and stimulation of the complement system through macrophages.[1] The antitumor and immunomodulatory properties are generally related to their ability to activate immune system.[2] The immune system is a system of many biological structures and processes within an organism that protects against disease. Most importantly, the macrophages occupy a unique position in the immune system because they can initiate natural immune responses and then act as effector cells that help manage immune responses,[3,4] such as inflammation, angiogenesis, and fighting an infection. Macrophages can eliminate the advanced stage of tumors because of their powerful functions, including phagocytosis and the release of numerous proinflammatory cytokines (interleukin), tumor necrosis factor, cytotoxic and inflammatory molecules (nitric oxide), and (reactive oxygen species) that contribute to direct and/or indirect antitumor activities.[5,6]

Our group recently isolated a novel polysaccharide from *Boletus speciosus* Frost (BSF-1), which has a backbone of (1 →4)-α-L-mannopyranose residues, which branches at O-6 and the branches were mainly composed of one with →1)-α-D-galactopyranose residue.[7] BSF-1 also exhibits significant antitumor activities *in vivo* and it can significantly promote the macrophage cells *in vitro*. However, the immunomodulatory activity and mechanism of BSF-1 remain unclear. Here, the goal of this study was to determine the molecular mechanisms underlying the immunomodulatory activity of BSF-1 in macrophages.

MATERIALS AND METHODS

Materials

The reagent 2-(2-methoxy-4-nitrophenyl-) 3-(4-nitrophenyl)-5-(2,4-disulfonic acid benzene)-2H-tetrazolium monosodium salt (Cell Counting Kit [CCK]-8) was purchased from Dojindo Molecular Technologies, Inc., (Tokyo, Japan); D-Hanks solution, RPMI 1640 medium, fetal calf serum, and dimethyl sulfoxide were purchased from Gibco (NY, USA). Penicillin G and streptomycin were purchased from Sigma (China). All other chemicals and solvents were of analytical grade, and BSF-1 was prepared in our laboratory as previously described.[7]

Cell lines and reagents

The RAW264.7 cell line, B (Raji) cell line, and T (Jurkat) cell line were cultured in RPMI 1640 medium containing 10% fetal bovine serum, 1% penicillin (100 IU/mL), and streptomycin (100 mg/L) in a humidified atmosphere with 5% CO_2 at 37°C before use.

Pharmacological evaluation for B-cells, T-cells, and RAW264.7 cells' stimulation

The cytotoxic effects of BSF-1 on B-cells, T–cells, and RAW264.7 cells were determined by CCK-8-based colorimetric method. In brief, B-cells, T–cells, and RAW264.7 cells suspended in RPMI-1640 medium at a density of 1×10^5 cells/ml were pipetted into a 96-well plate (100 μl/well) and inoculated at 37°C in a humidified 5% CO_2. After incubation for 24 h, 100 μl of test sample with different concentrations (0.3125–20 μg/mL in fresh growth medium) was added into each well separately in an incubator at 37°C in a humidified 5% CO_2 for 48 h. RPMI-1640 and 2 μg/mL lipopolysaccharides (LPS) were used as negative and positive controls, respectively. Then, 20 μl of CCK-8 reagent was added to each well, and the plate was further incubated for another 1–4 h. Absorbance of the colored solution at 490 nm was measured on a 96-well microplate reader (Bio-Rad, Tokyo, Japan). All experiments were performed in triplicate, and the inhibitory rate was calculated as follows:

Cell proliferation activity (%) = $[A2 - A0]/[A1 - A0] \times 100$

Where, $A2$ is the average optical density of BSF-1-treated cells, $A0$ is the average optical density of the control wells (culture medium without cells), and $A1$ is the average optical density of the negative control (culture medium containing cells).

Macrophage phagocytosis assay

The RAW264.7 cells were inoculated in the presence of varying concentrations of BSF-1 as mentioned above. RPMI-1640 and LPS were used as negative and positive controls, respectively. After 24 h, supernatants were removed, 100 μl of 0.075% neutral red solution was added to each well, and the cells were cultured for a further 1 h. And then, the plate was washed three times with phosphate-buffered saline (PBS) and patted gently on tissues to let them drain. Finally, 100 μl of cell lysis buffer (0.1 mol/L acetic acid and ethanol in the ratio of 1:1) was added to each well at 4°C for 2 h. The absorbance at 540 nm was determined using microplate ELISA reader. All determinations were conducted in triplicate.

RAW264.7 cell cycle analysis by flow cytometry

The effect of BSF-1 on the cell cycle distribution was assessed by flow cytometry after staining the cells with propidium iodide (PI). RAW264.7 cells were seeded in 6-well plates (5×10^5 cells/well) and allowed to grow for 1 day before being exposed to BSF-1 (1, 5, or 10 μg/mL) for 72 h. After incubation, the treated cells were harvested, washed twice with PBS, and fixed in cold 70% ethanol for 4 h or overnight at 4°C. After an additional wash in cold PBS, the cells were resuspended in 0.5 mL of staining buffer containing 10 μL of RNase and 25 μL of PI, and then incubated for 30 min in dark at 37°C. The DNA content of the cells was measured using a flow cytometer (BD, Franklin Lakes, NJ, USA), and the population of cells in each phase was calculated using the ModFit LT software (Verity Software House, Inc, NY, USA) program. Each experiment was conducted for three times.

RNA extraction, library preparation, and sequencing

TRIzol reagent (Invitrogen, Canada) was used to extract the total RNA, and 1% agarose gels were used to investigate the RNA contamination and degradation. RNA purity was detected on a Nano Photometer spectrophotometer (Implen, Westlake Village, CA, USA). After examining the RNA purity and concentration, the RNA 6000 Nano Assay Kit with NanoDrop2000 (Thermo Scientific NanoDrop 2000c) was used to assess the RNA integrity. A total of 3 μg of RNA per sample was used for the RNA sample preparations as input material.[8] Following the manufacturer's recommendations, the transcriptome libraries were generated using the Illumina TruSeq™ RNA Sample Preparation Kit (Illumina, San Diego, CA, USA). Clustering of the index-coded samples was completed using the TruSeq PE Cluster Kit v3-cBot-HS (Illumina) on a Bot Cluster Generation System. The libraries were sequenced on an Illumina HiSeq 2000 platform after clustering, and 100 bp paired-end reads were generated.[8]

Transcriptome data analysis

In-house Perl scripts were used to process the raw data in FASTQ format to remove low-quality reads, which contained poly-N stretches (partially un-sequenced regions) and adapter sequences. All the downstream analyses are based on the high-quality clean sequences.

Differential expression and quantification analysis of the transcripts

Prior to performing the differential gene expression analysis, the read counts were adjusted using an edgeR program package for each sequenced library through one scaling normalized factor. The reads per kilobase per million reads (RPKM) method was used to quantify the transcript expression, and HTSeq version 0.5.3 (European Molecular

Biology Laboratory (EMBL), Heidelberg, Germany) was used to count the number of reads mapped to each transcript. The RPKM value was calculated based on the mapped transcript fragments, sequencing depth, and transcript length.[8] The edgeR Bioconductor was used to complete the read counts with one scaling normalized factor before the analysis of differential gene expression, which was completed using the DEGseq R package, release 1.12.0. A log2-fold change of ± 1 and $P = 0.005$ were set as the threshold of statistically significant differential expression. A large fold-change value (|log2-fold-change| >5) was also used to identify differentially expressed genes (DEGs).

Gene ontology annotation and gene ontology/ Kyoto Encyclopedia of Genes and Genomes enrichment analyses

The protein functions of all the genes were annotated using BLASTX and InterProScan against the NCBI database. The resulting BLAST and InterPro annotations were then converted into gene ontology (GO) annotations. All the GO terms were mapped to the GO slim categories. Fisher's exact test within Blast2GO (false discovery rate [FDR] <0.05) was used to determine the statistical significance of the functional GO slim enrichment. A hyper geometric test and the Benjamini–Hochberg FDR correction were used to identify significantly enriched Kyoto Encyclopedia of Genes and Genomes (KEGG) pathways with KEGG Orthology-based Annotation System version 2.0 (KOBAS 2.0) (Peking University, Beijing, China).[8]

RESULTS AND DISCUSSION

Effect of *Boletus speciosus* Forst-1 on B-cell activation *in vitro*

B-cells, also known as B-lymphocytes, are a type of white blood cell of the lymphocyte subtype. They function in the humoral immunity component of the adaptive immune system by secreting antibodies. The stimulation of BSF-1 on B-cells is shown in Figure 1. Cell proliferation activity was lowest when B-cells were exposed to medium alone, whereas incubation of these cells with increasing concentrations of BSF-1 was associated with a dose-dependent increase in cell proliferation activity. Compared with the control group, the low concentration of BSF-1 significantly promoted B-cell proliferation (0.625–20 μg/mL, $^{**}P < 0.01$). Furthermore, cell proliferation activity at 1.25 μg/mL concentration of BSF-1 was comparable to or even greater than that elicited by 5 μg/mL LPS.

Effect of *Boletus speciosus* Forst-1 on T-cell activation *in vitro*

T-cells are a type of lymphocyte which plays a central role in cell-mediated immunity. They can be distinguished from other lymphocytes, such as B-cells and natural killer cells, by the presence of a T-cell receptor on the cell surface. They are called T-cells because they mature in the thymus from thymocytes. The stimulation of BSF-1 on T-cells is shown in Figure 2. Compared with the control group, the low concentration of BSF-1 significantly promoted T-cell proliferation (1.25 μg/mL, $^{*}P < 0.05$; 2.5–20 μg/mL, $^{**}P < 0.01$). Cell proliferation activity at 2.5 μg/mL concentration of BSF-1 was comparable to or even greater than that elicited by 5 μg/mL LPS.

Effect of *Boletus speciosus* Forst-1 on macrophage activation *in vitro*

Macrophages are a type of white blood cell that engulfs and digests cellular debris, foreign substances, microbes, cancer cells, and anything else that does not have the types of proteins specific of healthy body cells on its surface in a process called phagocytosis. The stimulation of BSF-1 on macrophage is shown in Figure 3. Compared with the control group,

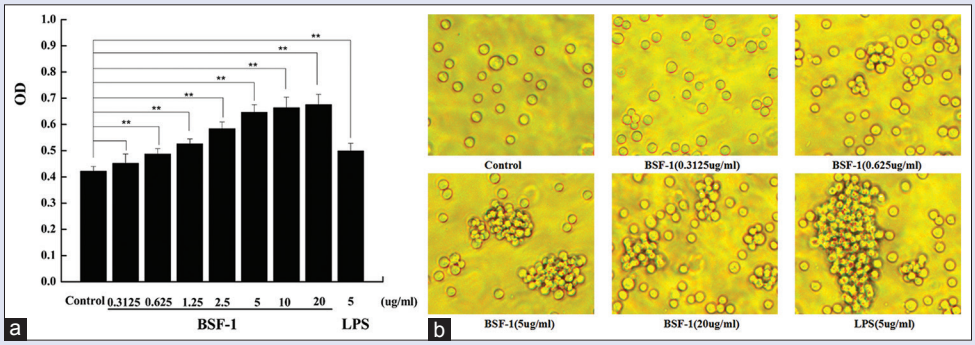

Figure 1: (a) Effects of *Boletus speciosus* Frost-1 on the proliferation of B-cells *in vitro*. (b) Morphological observation of B-cells

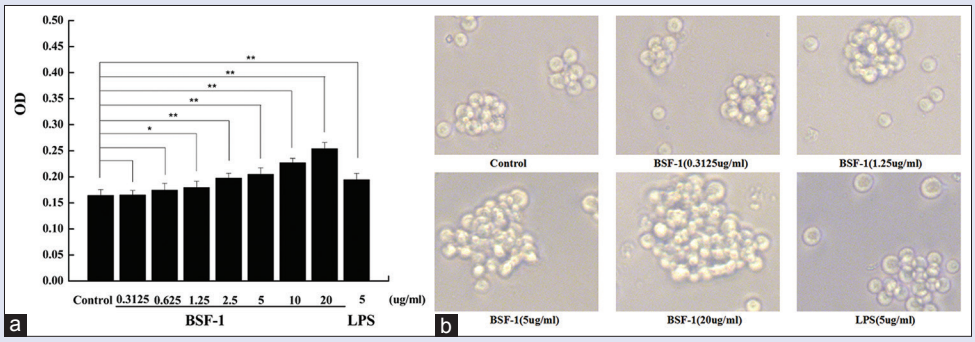

Figure 2: (a) Effects of *Boletus speciosus* Frost-1 on the proliferation of T-cells *in vitro*. (b) Morphological observation of T-cells

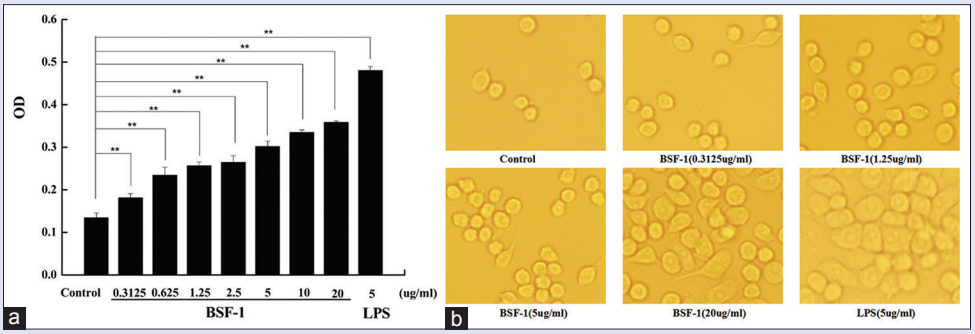

Figure 3: (a) Effects of *Boletus speciosus* Frost-1 on the proliferation of RAW264.7 cells *in vitro*. (b) Morphological observation of RAW264.7 cells

the low concentration of BSF-1 significantly promoted RAW264.7 cell proliferation (0.3125–20 μg/mL, $^{**}P < 0.01$). It is worth noting that cell proliferation activity at 20 μg/mL concentration of BSF-1 was lower than that elicited by 5 μg/mL LPS.

Macrophage phagocytosis

One of the most distinguished features of macrophage activation would be an increase in pinocytic activity. Pinocytic activity of BSF-1-activated macrophages was examined by the uptake of neutral red (0.075%). From Figure 4, it can be observed that after 24 h incubation with varying concentrations of BSF-1, the BSF-1 enhanced the phagocytic activity of RAW264.7 in the testing dose range with a dose-dependent way compared to the negative control. Furthermore, pinocytic activity at 0.3125–20 μg/mL concentrations of BSF-1 was comparable to or even greater than that elicited by 5 μg/mL LPS, a positive control.

Effects of *Boletus speciosus* Forst-1 on the cell cycle distribution of RAW264.7 cells

The cell cycle analysis was performed on RAW264.7 cells using flow cytometry to examine the effects of BSF-1 on cell cycle progression. Figure 5 shows the effects of BSF-1 on the cell cycle phase (G0/G1, S, and G2/M) distribution of RAW264.7 cells using flow cytometry with PI staining. The treatment of RAW264.7 cells with BSF-1 at 10 μg/mL for 72 h induced a concentration-dependent increase in the G2/M phase population from 15.7% of the control group to 19.5% of the BSF-1 group ($P < 0.05$ or $P < 0.01$), with a concomitant decrease in the percentage of cells in the G0/G1 phase from 71.9% of the control group to 66.3% of the BSF-1 group. At the tested concentrations, BSF-1 also induced a significant change in the S-phase population, from 13.2% of the control group to 15.2% of the BSF-1 group. These results suggested that BSF-1 could promote the proliferation of macrophage cells by abolishing cell cycle arrests in the G0/G1 phase and promote cell cycle progression in S-phase and G2/M phase, which might induce cell division.

Transcriptome sequencing and *de novo* assembly

High-throughput and low-cost next-generation sequencing technologies, such as RNA-Seq, have become popular and useful not only for *de novo* genome assembly and genome diversity studies, but also to investigate gene expression profiles and discover pharmacological activity mechanisms. In our previous studies, the polysaccharide BSF-1 exhibited significant antitumor activities *in vivo*. The inhibitory rate in mice treated with 40 mg/kg BSF-1 reached 62.449%, which might be comparable to the effects of mannatide. However, the immunomodulatory activity and mechanism of BSF-1 remain unclear. To explore differences in the RAW264.7 cell transcriptomes between the control group and the BSF-1 group, two cell groups were selected for analysis. Two cDNA libraries

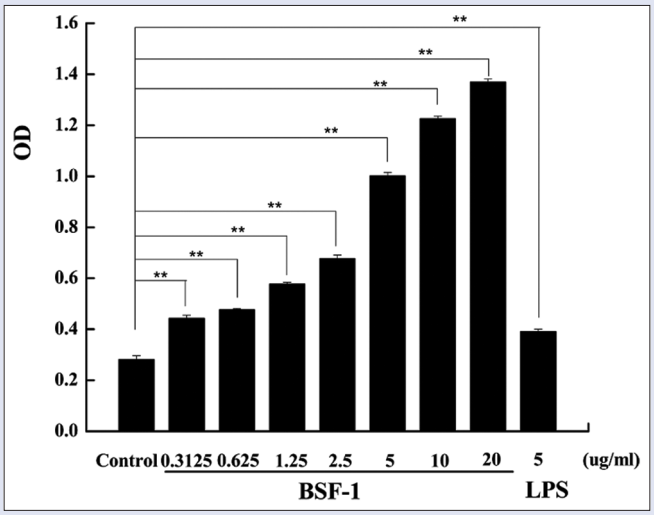

Figure 4: Effects of *Boletus speciosus* Frost-1 on the phagocytic activity of RAW264.7 cells *in vitro*

were constructed with the respective total RNA from the control and BSF-1 groups. The prepared libraries were sequenced on an Illumina HiSeq 2000 platform. After quality control, a total of 12,498,414 and 11,840,624 bp paired-end reads were obtained for the control and BSF-1 groups, respectively, which corresponded to a total size of 12.5 G bp and 11.8 G bp, respectively, after the low-quality reads and adapter sequences were removed [Table 1 and Figure 6]. We mapped the clean reads to the RAW264.7 cell reference genome. The proportion of total reads in the two RAW264.7 cell transcriptome libraries that mapped to the genome ranged from 41.04% to 40.03%. A sequencing saturation analysis showed that the number of genes detected by the library was saturated [Figure 7]. A 5'-3' sequence preference statistical analysis showed that the sequencing was mainly focused on the gene body region, and the bias at the two ends was limited [Figure 8]. The distribution of gene coverage is shown in Figure 9 and it provides a good basis for the follow-up analysis.

Transcriptome profiles of the two RAW264.7 cell groups

The abundance of all the genes was calculated and normalized using uniquely mapped reads by the RPKM method. The distribution of the expression levels of all the genes was similar for the two groups. Genes with RPKMs over 60 were considered to be expressed at a high level, whereas genes with RPKMs in the interval of 0–1 were considered to be expressed at low levels or not at all. The results showed that in the

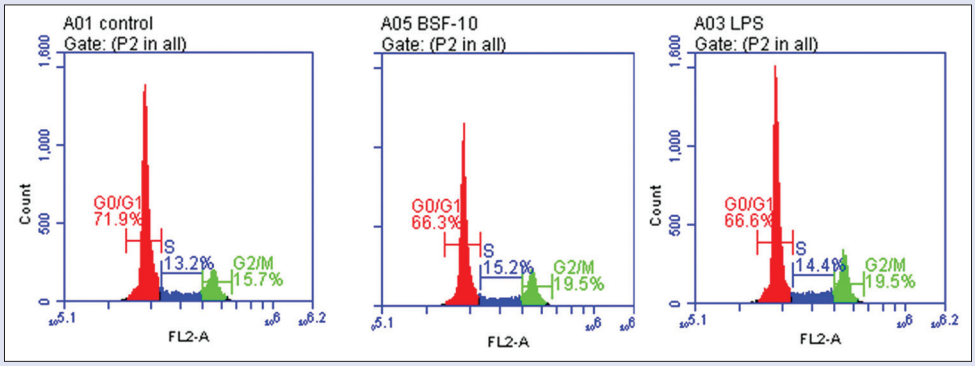

Figure 5: Effects of *Boletus speciosus* Frost-1 on macrophage cycle

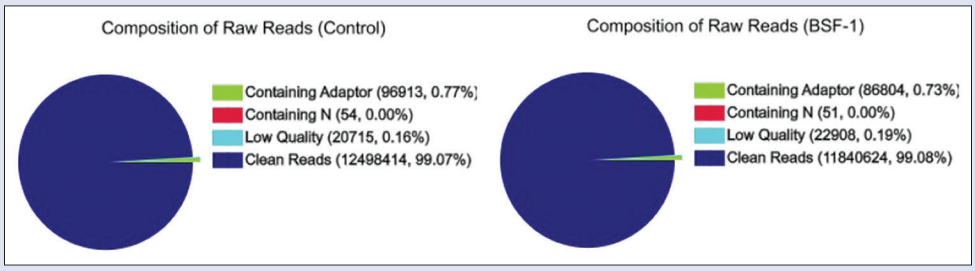

Figure 6: Quality assessment of the reads

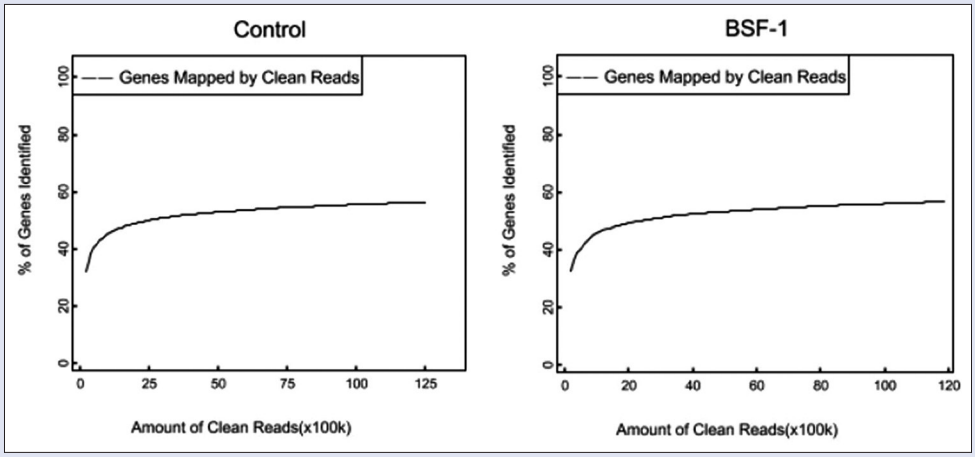

Figure 7: Sequencing saturation analysis

Table 1: Summary of the mapping results (mapping to reference genome)

Sample ID	Total reads (%)	Total base pairs (%)	Total mapped reads (%)	Perfect match (%)	≤2 bp mismatch (%)	Unique match (%)	Multi-position match (%)	Total unmapped reads (%)
Control	12,498,414 (100.00)	612,422,286 (100.00)	5,129,004 (41.04)	985,094 (7.88)	4,143,910 (33.16)	3,166,326 (25.33)	1,962,678 (15.70)	7,369,410 (58.96)
BSF-1	11,840,624 (100.00)	580,190,576 (100.00)	4,739,212 (40.03)	896,331 (7.57)	3,842,881 (32.46)	2,988,159 (25.24)	1,751,053 (14.79)	7,101,412 (59.97)

BSF-1: *Boletus speciosus* Frost-1

control group, approximately 81.77% of the total number of genes (8208) were expressed (RPKM ≥1) and more than 1333 genes were highly expressed (RPKM >60), whereas in the BSF-1 group, approximately 81.83% of the total number of genes (8257) were expressed (RPKM ≥1) and more than 1366 genes were highly expressed (RPKM >60). The results also showed that eight genes (Rps6, Tpt1, Rpl23, Eef1α1, Fth1, Rpl5, Rps24, and Rplp2) were extremely highly expressed (RPKM >10,000) in the control group [Table 2], whereas nine genes (Eef1a1, Fth1, Rpl23, Rps24, Tpt1, Rps6, Rpl5, Rplp2, and Rps27) were extremely highly expressed (RPKM >9000) in the BSF-1 group [Table 3]. It is worth noting that the RPKM of the Eef1a1 gene was 27073.88 in the control group and 26186.717 in the BSF-1 group.

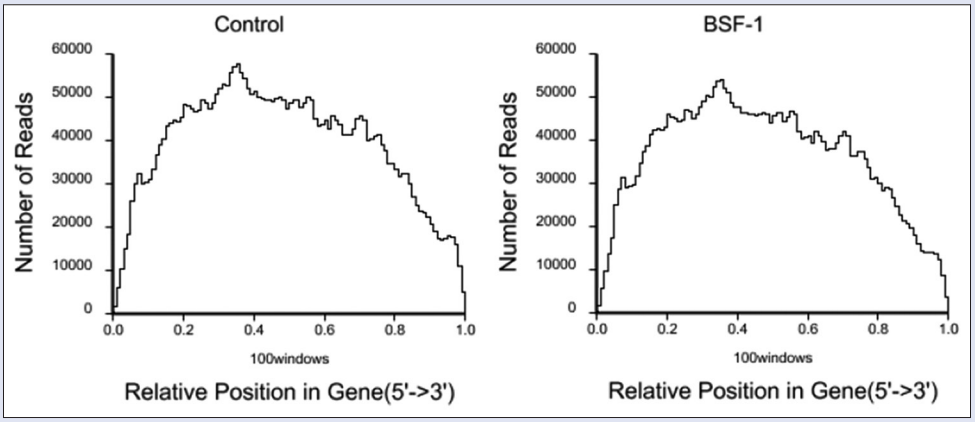

Figure 8: Randomness assessment

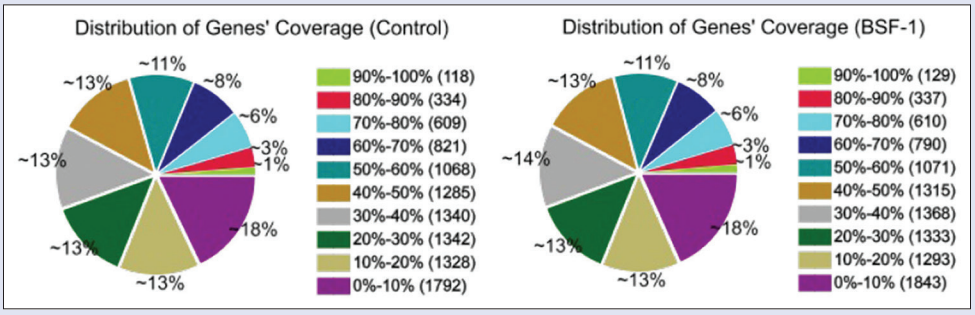

Figure 9: Distribution of gene coverage

Table 2: Quantification of gene expression in the control group (reads per kilobase per million reads >10,000)

Gene ID	Uniq_reads_num	Length	Coverage (%)	RPKM	Symbol	Description	KEGG Orthology
171361	175,276	1737	97.64	27,073.88	Eef1a1	Eukaryotic translation elongation factor 1 alpha 1	K03231
25319	49,515	828	99.88	16,044.80	Fth1	Ferritin, heavy polypeptide 1	K00522
81763	40,233	1069	92.33	10,097.94	Rpl5	Ribosomal protein L5	K02932
29304	39,202	801	82.90	13,131.18	Rps6	Ribosomal protein S6	K02991
116646	35,323	794	95.59	11,936.17	Tpt1	Tumor protein, translationally controlled 1	-
29282	29,570	518	89.38	15,316.15	Rpl23	Ribosomal protein L23	K02894
81776	24,758	466	93.56	14,254.68	Rps24	Ribosomal protein S24	K02974
1406	19,179	453	86.31	11,359.41	Rplp2	Ribosomal protein, large P2	K02943

KEGG: Kyoto Encyclopedia of Genes and Genomes; RPKM: Reads per kilobase per million mapped reads

Table 3: Quantification of gene expression in the *Boletus speciosus* Frost-1 group (reads per kilobase per million reads >9000)

Gene ID	Uniq_reads_num	Length	Coverage (%)	RPKM	Symbol	Description	KEGG Orthology
171361	157,237	1737	97.29	26,186.717	Eef1a1	Eukaryotic translation elongation factor 1 alpha 1	K03231
25319	42,696	828	99.88	14,917.051	Fth1	Ferritin, heavy polypeptide 1	K00522
29282	26,175	518	89.77	14,617.835	Rpl23	Ribosomal protein L23	K02894
81776	21,988	466	93.78	13,649.789	Rps24	Ribosomal protein S24	K02974
116646	31,404	794	95.34	11,441.701	Tpt1	Tumor protein, translationally controlled 1	-
29304	30,870	801	82.77	11,148.854	Rps6	Ribosomal protein S6	K02991
81763	35,537	1069	93.36	9616.769	Rpl5	Ribosomal protein L5	K02932
140662	14,773	453	96.91	9434.016	Rplp2	Ribosomal protein, large P2	K02943
94266	11,809	366	89.34	9333.793	Rps27	Ribosomal protein S27	K02978

KEGG: Kyoto Encyclopedia of Genes and Genomes; RPKM: Reads per kilobase per million mapped reads

Differentially expressed genes between the control and *Boletus speciosus* Forst-1 groups

The reads were adjusted using the edgeR program with one scaling normalized factor, and the DEGs between the two cell groups were identified using the DEGSeq R package. Values of FDR ≤0.001 and |log2 Ratio| ≥1 were set as the thresholds for significant differential expression. Our research group performed hierarchical clustering for all the DEGs based on the log10 RPKMs of the two cell groups to observe the gene expression patterns [Figure 10]. A total of 13 unigenes were identified

as DEGs, and approximately 5 genes were upregulated, whereas 8 genes were downregulated [Figure 10], which might have contributed to the proliferation and phagocytic activities of RAW264.7 cells following BSF-1 treatment *in vitro*. The number of DEGs in the control versus BSF-1 were 12 for transcripts detected with | log2-fold-change| >1 and 3 for transcripts detected with | log2-fold-change| >2. Among the DEGs within the | log2-fold-change| >1 threshold, 4 genes were upregulated, including Trim23, Znhit6, Lamc1, and Zbtb7a, among others, whereas 8 genes were downregulated, including LOC100360880, Dusp1, Fos, Zfp36, Ier3, Ier2, Atp6v0d2, and Cars [Tables 4 and 5].

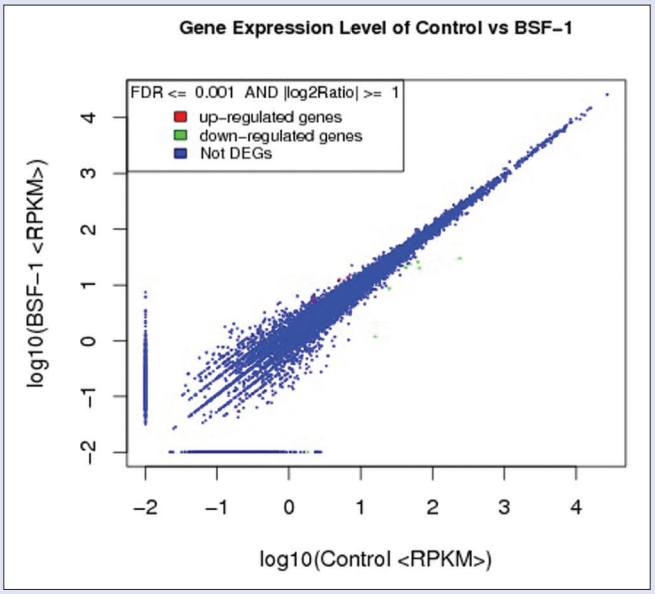

Figure 10: Scatter plot of differential expression

Gene ontology and Kyoto Encyclopedia of Genes and Genomes enrichment analyses of the differentially expressed genes

GO analyses were used to confirm the functional classifications of the annotated unigenes and classify the transcripts with known proteins. A total of 39,271 genes were annotated with GO terms, which were converted into generic GO slim terms. The GO enrichment analysis was performed using Fisher's exact test in Blast2GO to analyze the gene functions of the DEGs. The analysis generated 13,042 assignments to cellular components, 13,094 assignments to biological processes, and 13,135 assignments to molecular functions [Figure 11]. In the category of cellular components, 96.60% and 96.60% of the unigenes were located in cell parts (GO: 0044464) and cells (GO: 0005623), respectively. Under the molecular functions, the majority of the GO terms were grouped into intracellular part (GO: 0044424), intracellular (GO: 0005622), intracellular membrane-bounded organelle (GO: 0043231), membrane-bounded organelle (GO: 0043227), intracellular organelle (GO: 0043229), and organelle (GO: 0043226) [Table 6]. These results suggested that the immune mechanisms may present additional differences between the control and BSF-1 groups.

The pathway analysis was conducted using the KEGG pathway database to further understand the biological function of the gene products. The KEGG pathway enrichment analysis was performed using KOBAS. A KEGG analysis records the molecular interaction networks in cells with variants that are specific to particular organism. Our analysis identified 22.22% DEGs in the mitogen-activated protein kinase (MAPK) signaling pathway [Figure 12], including MKP (K04459: 114856) and c-fos (K04379: 314322). The MAPK signaling cascade is a common signal transduction module that connects different receptors/sensors to nuclear and cellular responses. The classical MAPK signaling cascade consists of three types of phosphorylated kinases: MAPK, MAPK kinase (MAPKK/MEK), and MAPKK kinase (MAPKKK/MEKK).[9] In the

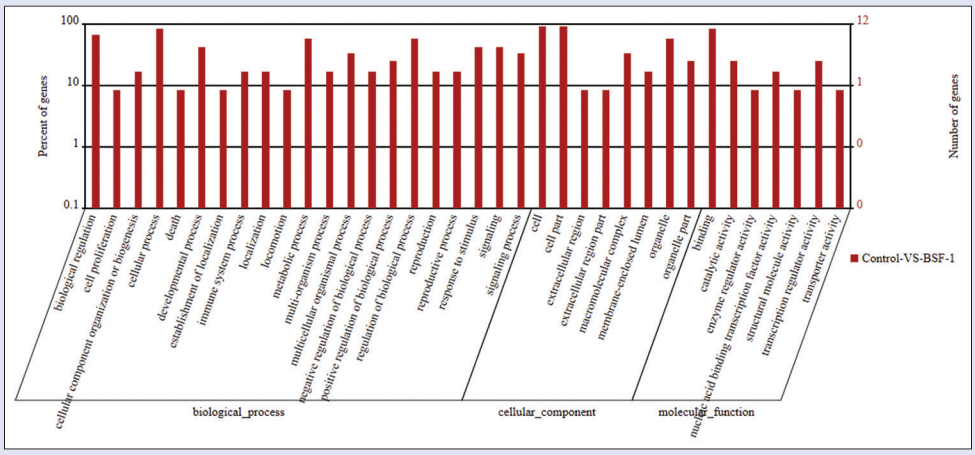

Figure 11: Gene ontology functional classification of the differentially expressed genes

Table 4: Differentially expressed genes: Upregulated (|log2-fold-change| > 1)

Gene ID	Gene_length	log2 ratio (BSF-1/control)	Symbol	Description	KEGG Orthology
81002	3308	1.483016642	Trim23	Tripartite motif-containing 23	K07963
292160	1586	1.310254989	Znhit6	Zinc finger, HIT-type containing 6	-
117036	7636	1.131341204	Lamc1	Laminin, gamma 1	K05635
117107	2817	1.024963199	Zbtb7a	Zinc finger and BTB domain containing 7a	K10494

BSF-1: *Boletus speciosus* Frost-1; KEGG: Kyoto Encyclopedia of Genes and Genomes

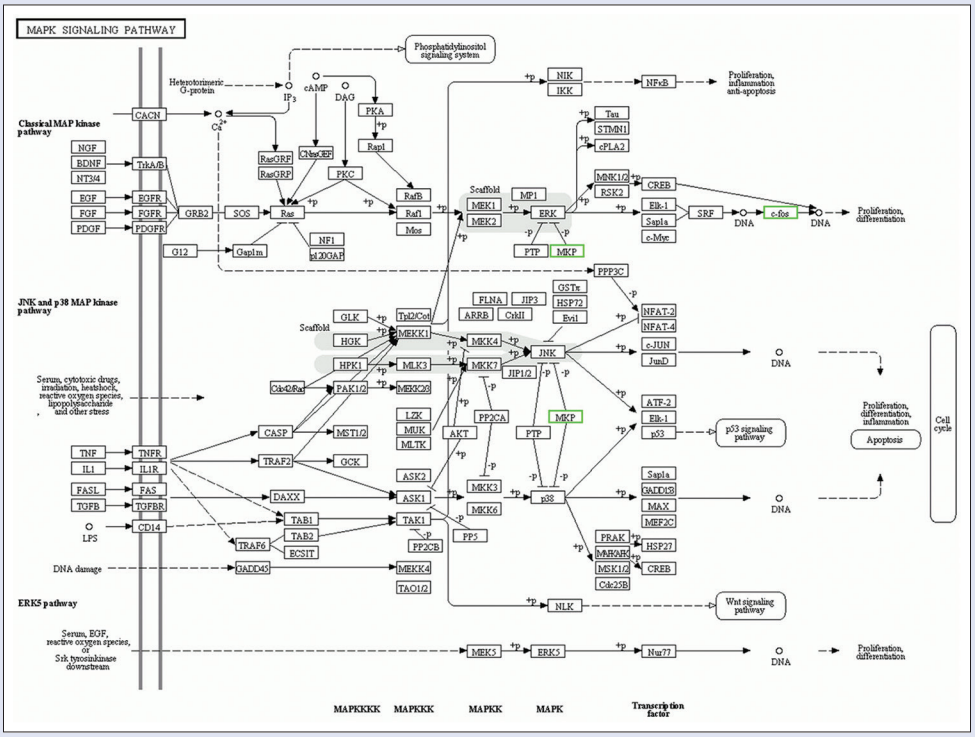

Figure 12: Mitogen-activated protein kinase signaling pathway

Table 5: Differentially expressed genes: Downregulated (|log2-fold-change| > 1)

Gene ID	Gene_length	log2 ratio (BSF-1/Control)	Symbol	Description	KEGG Orthology
100360880	3251	−7.504347241	LOC100360880	FBJ osteosarcoma oncogene B	K09029
114856	1940	−3.736868923	Dusp1	Dual specificity phosphatase 1	K04459
314322	1589	−2.982925779	Fos	FBJ osteosarcoma oncogene	K04379
79426	1811	−1.713497147	Zfp36	Zinc finger protein 36	K15308
294235	1114	−1.547424471	Ier3	Immediate early response 3	-
494344	1564	−1.298554254	Ier2	Immediate early response 2	-
297932	1330	−1.07331925	Atp6v0d2	ATPase, H+transporting, lysosomal V0 subunit D2	K02146
293638	2970	−1.02032673	Cars	Cysteinyl-tRNA synthetase	K01883

FBJ: Finkel-Biskis-Jinkins; BSF-1: *Boletus speciosus* Frost-1; KEGG: Kyoto Encyclopedia of Genes and Genomes

Table 6: Gene ontology enrichment analysis of the differentially expressed genes

Gene ontology term	Cluster frequency	Genome frequency of use	Corrected *P* value
Cell - GO: 0005623	11 out of 12 genes, 91.7%	12,602 out of 13,042 genes, 96.6%	1
Cell part - GO: 0044464	11 out of 122 genes, 91.7%	12,602 out of 13,042 genes, 96.6%	1
Intracellular part - GO: 0044424	10 out of 12 genes, 83.3%	9289 out of 13,042 genes, 71.2%	1
Intracellular - GO: 0005622	10 out of 12 genes, 83.3%	9321 out of 13,042 genes, 71.5%	1
Intracellular membrane-bounded organelle - GO: 0043231	7 out of 12 genes, 58.3%	7081 out of 13,042 genes, 54.3%	1
Membrane-bounded organelle - GO: 0043227	7 out of 12 genes, 58.3%	7169 out of 13,042 genes, 55.0%	1
Intracellular organelle - GO: 0043229	7 out of 12 genes, 58.3%	7819 out of 13,042 genes, 60.0%	1
Organelle - GO: 0043226	7 out of 12 genes, 58.3%	7918 out of 13,042 genes, 60.7%	1

GO: Gene ontology

MAPK signaling pathway, epidermal growth factor (EGF) acts by binding to EGF receptors on the cell surface, which leads to cell proliferation, differentiation, and survival. This process stimulates ligand dimerization and starts a signal transduction cascade reaction that results in a series of biochemical changes in cells as well as increased intracellular calcium levels, glycolysis, and protein synthesis, with these changes eventually causing cell proliferation and DNA synthesis.[4,9-16] This process would adequately explain the mechanism of BSF-1's proliferation activity on macrophages.

It is worth noting that the phagosome and oxidative phosphorylation (11.11% DEGs with pathway annotation,respectively) between the two cell groups is also enriched for DEGs. These results indicated that BSF-1 could promote the proliferation of macrophage cells by abolishing cell cycle arrests and might induce cell division.

CONCLUSION

Our results suggested that BSF-1 could promote the proliferation of B-cells, T-cells, and macrophages, promote the proliferation of macrophage cells by abolishing cell cycle arrests in the G0/G1 phase, and promote cell cycle progression in S-phase and G2/M phase, which might induce cell division. A total of 12,498,414 and 11,840,624 bp paired-end reads were obtained for the control and BSF-1 groups, respectively, and they corresponded to a total size of 12.5 G bp and 11.8 G bp, respectively, after the low-quality reads and adapter sequences were removed. Approximately 81.83% of the total number of genes (8257) were expressed (RPKM ≥1) and more than 1366 genes were highly expressed (RPKM >60) in the BSF-1 group. A GO enrichment analysis generated 13,042 assignments to cellular components, 13,094 assignments to biological processes, and 13,135 assignments to molecular functions. A KEGG pathway enrichment analysis showed that the MAPK signaling pathways are significantly enriched for DEGs between the two cell groups. An analysis of transcriptome resources enabled us to examine gene expression profiles, verify differential gene expression, and select candidate signaling pathways as the mechanisms of the immunomodulatory activity of BSF-1. Based on the experimental data and the results from our previous work, we believe that the significant antitumor activities of BSF-1 *in vivo* may involve the MAPK signaling pathway. Our results provide a foundation for understanding the molecular mechanisms underlying the antitumor activity and immune activity of polysaccharides.

Acknowledgements

This study was supported by the National Natural Science Foundation of China, Sichuan Province of China, Guizhou Province of China, and China West Normal University.

Financial support and sponsorship

This study was supported by the National Natural Science Foundation of China (31400016 and 31200012), the Application Foundation Project of Sichuan Province (2013JY0094), the Science and Technology Support Project of Sichuan Province (2014SZ0020 and 2014FZ0024), the Cultivate Major Projects of Sichuan Province (14CZ0016 and 16CZ0018), the Open Foundation of Microbial Resources and Drug Development of Key Laboratory of Guizhou Province (GZMRD-2014-002), and the Doctor Startup Foundation Project of China West Normal University (11B019 and 11B020).

Conflicts of interest

There are no conflicts of interest.

REFERENCES

1. Cheng A, Wan F, Wang J, Jin Z, Xu X. Macrophage immunomodulatory activity of polysaccharides isolated from *Glycyrrhiza uralensis* Fish. Int Immunopharmacol 2008;8:43-50.
2. Zhao Z, Li J, Wu X, Dai H, Gao X, Liu M, *et al.* Structures and immunological activities of two pectic polysaccharides from the fruits of *Ziziphus jujuba* Mill. cv. jinsixiaozao Hort. Food Res Int 2006;39:917-23.
3. Lee KY, Jeon YJ. Macrophage activation by polysaccharide isolated from *Astragalus membranaceus*. Int Immunopharmacol 2005;5:1225-33.
4. Song JY, Han SK, Son EH, Pyo SN, Yun YS, Yi SY. Induction of secretory and tumoricidal activities in peritoneal macrophages by ginsan. Int Immunopharmacol 2002;2:857-65.
5. Ma H, Liu G, Ding W, Wu Y, Cai L, Zhao Y. Diabetes-induced alteration of F4/80+macrophages: A study in mice with streptozotocin-induced diabetes for a long term. J Mol Med (Berl) 2008;86:391-400.
6. Di Carlo E, Forni G, Lollini P, Colombo MP, Modesti A, Musiani P. The intriguing role of polymorphonuclear neutrophils in antitumor reactions. Blood 2001;97:339-45.
7. Ding X, Hou Y, Hou W. Structure feature and antitumor activity of a novel polysaccharide isolated from *Lactarius deliciosus* Gray. Carbohydr Polym 2012;89:397-402.
8. Fang SM, Hu BL, Zhou QZ, Yu QY, Zhang Z. Comparative analysis of the silk gland transcriptomes between the domestic and wild silkworms. BMC Genomics 2015;16:60.
9. Orton RJ, Sturm OE, Vyshemirsky V, Calder M, Gilbert DR, Kolch W. Computational modelling of the receptor-tyrosine-kinase-activated MAPK pathway. Biochem J 2005;392(Pt 2):249-61.
10. Herbst RS. Review of epidermal growth factor receptor biology. Int J Radiat Oncol Biol Phys 2004;59 2 Suppl: 21-6.
11. Zarubin T, Han J. Activation and signaling of the p38 MAP kinase pathway. Cell Res 2005;15:11-8.
12. Razali FN, Ismail A, Abidin NZ, Shuib AS. Stimulatory effects of polysaccharide fraction from *Solanum nigrum* on RAW 264.7 murine macrophage cells. PLoS One 2014;9:e108988.
13. Rein DT, Kurbacher CM. The role of chemotherapy in invasive cancer of the cervix uteri: Current standards and future prospects. Anticancer Drugs 2001;12:787-95.
14. Schepetkin IA, Quinn MT. Botanical polysaccharides: Macrophage immunomodulation and therapeutic potential. Int Immunopharmacol 2006;6:317-33.
15. Shin JY, Song JY, Yun YS, Yang HO, Rhee DK, Pyo S. Immunostimulating effects of acidic polysaccharides extract of *Panax ginseng* on macrophage function. Immunopharmacol Immunotoxicol 2002;24:469-82.
16. Song G, Du Q. Structure characterization and antitumor activity of an α β-glucan polysaccharide from auricularia polytricha. Food Res Int 2012;45:381-7.